Adenosine A_1-A_{2A} Receptor-Receptor Interaction: Contribution to Guanosine-Mediated Effects

Débora Lanznaster [1,†], **Caio M. Massari** [2,†], **Vendula Marková** [3,4], **Tereza Šimková** [3,4], **Romain Duroux** [5], **Kenneth A. Jacobson** [5], **Víctor Fernández-Dueñas** [3,4,*], **Carla I. Tasca** [1,6,*] **and Francisco Ciruela** [3,4,*]

1. Programa de Pós-graduação em Neurociências, Centro de Ciências Biológicas, Universidade Federal de Santa Catarina, 88040-900 Florianópolis, Brazil; de_lanz@hotmail.com
2. Programa de Pós-graduação em Bioquímica, Centro de Ciências Biológicas, Universidade Federal de Santa Catarina, 88040-900 Florianópolis, Brazil; caio.massari@gmail.com
3. Unitat de Farmacologia, Departament de Patologia i Terapèutica Experimental, Facultat de Medicina i Ciències de la Salut, IDIBELL, Universitat de Barcelona, 08907 L'Hospitalet de Llobregat, Spain; Vendy.Markova@seznam.cz (V.M.); simkovat@gmail.com (T.Š.)
4. Institut de Neurociències, Universitat de Barcelona, 08035 Barcelona, Spain
5. Molecular Recognition Section, Laboratory of Bioorganic Chemistry, National Institute of Diabetes and Digestive and Kidney Diseases, National Institutes of Health, Bethesda, MD 20892, USA; Romain.Duroux@niddk.nih.gov (R.D.); kennethj@niddk.nih.gov (K.A.J.)
6. Departamento de Bioquímica, Centro de Ciências Biológicas, Universidade Federal de Santa Catarina, 88040-900 Florianópolis, Brazil
* Correspondence: vfernandez@ub.edu (V.F.-D.); carla.tasca@ufsc.br (C.I.T.); fciruela@ub.edu (F.C.); Tel.: +34-934-024-280 (F.C.)
† These authors contributed equally to this work.

check for updates

Abstract: Guanosine, a guanine-based purine nucleoside, has been described as a neuromodulator that exerts neuroprotective effects in animal and cellular ischemia models. However, guanosine's exact mechanism of action and molecular targets have not yet been identified. Here, we aimed to elucidate a role of adenosine receptors (ARs) in mediating guanosine effects. We investigated the neuroprotective effects of guanosine in hippocampal slices from $A_{2A}R$-deficient mice ($A_{2A}R^{-/-}$) subjected to oxygen/glucose deprivation (OGD). Next, we assessed guanosine binding at ARs taking advantage of a fluorescent-selective $A_{2A}R$ antagonist (MRS7396) which could engage in a bioluminescence resonance energy transfer (BRET) process with NanoLuc-tagged $A_{2A}R$. Next, we evaluated functional AR activation by determining cAMP and calcium accumulation. Finally, we assessed the impact of A_1R and $A_{2A}R$ co-expression in guanosine-mediated impedance responses in living cells. Guanosine prevented the reduction of cellular viability and increased reactive oxygen species generation induced by OGD in hippocampal slices from wild-type, but not from $A_{2A}R^{-/-}$ mice. Notably, while guanosine was not able to modify MRS7396 binding to $A_{2A}R$-expressing cells, a partial blockade was observed in cells co-expressing A_1R and $A_{2A}R$. The relevance of the A_1R and $A_{2A}R$ interaction in guanosine effects was further substantiated by means of functional assays (i.e., cAMP and calcium determinations), since guanosine only blocked $A_{2A}R$ agonist-mediated effects in doubly expressing A_1R and $A_{2A}R$ cells. Interestingly, while guanosine did not affect $A_1R/A_{2A}R$ heteromer formation, it reduced $A_{2A}R$ agonist-mediated cell impedance responses. Our results indicate that guanosine-induced effects may require both A_1R and $A_{2A}R$ co-expression, thus identifying a molecular substrate that may allow fine tuning of guanosine-mediated responses.

Keywords: guanosine; neuroprotection; oxygen/glucose deprivation; NanoBRET; $A_1R/A_{2A}R$ heteromer

1. Introduction

Guanosine is a guanine-based purine nucleoside that has been shown to exert neuroprotective and neurotrophic effects in both in vitro and in vivo studies (for review, see [1]). Thus, it has been postulated as a good candidate for the management of several central nervous system (CNS) disorders, including neurodegenerative diseases (i.e., Parkinson's, Alzheimer's) or ischemia [1,2]. Brain ischemia is one of the major health disability conditions worldwide [3]. It occurs after a blood supply collapse that leads to a reduced level of oxygen and glucose within the affected brain area. Similarly, upon excitotoxicity and oxidative stress a failure of cellular bioenergetics occurs [4]. Importantly, a neuroprotective role of guanosine has been extensively investigated in animal and cellular models of ischemia, excitotoxicity and oxidative stress [5–10]. Indeed, we have demonstrated that guanosine prevents reactive oxygen species (ROS) generation and cell death in hippocampal slices subjected to the oxygen/glucose deprivation (OGD) [11].

The mechanism by which guanosine exerts its neuroprotective effects is still intriguing. Despite the identification of a putative guanosine binding site in rat brain membranes [12], a specific guanosine receptor has not yet been discovered. Importantly, it has been hypothesized that adenosine receptors (ARs) may play a role in mediating guanosine effects, although with some controversy. For instance, it has been reported that AR selective ligands do not compete for guanosine binding to rat brain membranes [13,14], whereas AR ligands were able to block some of the guanosine-dependent neuroprotective effects [15]. In line with this, a selective adenosine A_1 receptor (A_1R) antagonist (DPCPX, 8-cyclopentyl-1,3-dipropylxanthine) and a selective A_{2A} receptor (A_{2A}R) agonist (CGS21680, 2-(4-(2-carboxyethyl)phenethylamino)-5'-*N*-ethylcarboxamidoadenosine) inhibited guanosine-mediated neuroprotection in hippocampal slices subjected to OGD [11]. Overall, these findings, including those using multimodal A_1R and A_{2A}R ligand treatments, supported the notion that both A_1R and A_{2A}R would participate in guanosine-mediated effects.

Interestingly, it has been hypothesized that adenosine A_1 and A_{2A} receptor-receptor interactions (i.e., heteromerization) might be behind some of the guanosine-mediated effects, thus pointing to the A_1R/A_{2A}R heteromer as a putative molecular target for guanosine [16]. Indeed, the existence of A_1R/A_{2A}R heteromers has been demonstrated in presynaptic terminals of striatal neurons controlling glutamate release [17], thus acting as an adenosine concentration-dependent switch [18]. Consequently, low to moderate concentrations of adenosine predominantly activate A_1R within the A_1R/A_{2A}R heteromer (i.e., inhibiting glutamate release), whereas moderate to high concentrations of adenosine also activate A_{2A}R, which, by means of the A_1R-A_{2A}R intramembrane negative allosteric interaction, antagonizes A_1R function, therefore facilitating glutamate release. Altogether, in view of the already known experimental indications, the A_1R/A_{2A}R heteromer might be viewed as a potential target for guanosine, thus deserving further attention. Here, we aimed to assess the role of A_1R and A_{2A}R interaction in guanosine-mediated effects. First, we studied the neuroprotective effects of guanosine in an ex vivo model of brain ischemia, both in wild-type and A_{2A}R deficient ($A_{2A}R^{-/-}$) mice; subsequently, we aimed to elucidate, in vitro, both the putative guanosine binding and activation of the A_1R/A_{2A}R heteromer.

2. Materials and Methods

2.1. Chemicals

The ligands used were: adenosine and guanosine from Sigma-Aldrich (St. Louis, MO, USA); CGS21680 and SCH442416 (2-(2-furyl)-7-[3-(4-methoxyphenyl)propyl]-7*H*-pyrazolo [4,3-*e*]-[1,2,4]triazolo [1,5-*c*]pyrimidin-5-amine) from Tocris Bioscience (Ellisville, MI, USA). Adenosine deaminase (ADA) was purchased from Roche Diagnostics (GmbH, Mannheim, Germany) and zardaverine from Calbiochem (San Diego, CA, USA). MRS7396, which is a selective fluorescent antagonist at the A_{2A}R derived from SCH442416, was previously described [19].

2.2. Animals

Wild-type and $A_{2A}R^{-/-}$ CD-1 male and female mice [20] weighing 25–50 g were used at 2–3 months of age. The University of Barcelona Committee on Animal Use and Care (CEEA-UB) approved the protocol (Code 10033, 04/02/2018). Animals were housed and tested in compliance with the guidelines described in the Guide for the Care and Use of Laboratory Animals [21] and following the European Union directives (2010/63/EU), FELASA and ARRIVE guidelines. Mice were housed in groups of five in standard cages with ad libitum access to food and water and maintained under a 12-h dark/light cycle (starting at 7:30 AM), 22 °C temperature, and 66% humidity (standard conditions).

2.3. OGD Protocol

Mice were euthanized by cervical dislocation and hippocampi rapidly removed and placed in an ice-cold Krebs-Ringer bicarbonate buffer (KRB) (composition in mM: 122 NaCl, 3 KCl, 1.2 $MgSO_4$, 1.3 $CaCl_2$, 0.4 KH_2PO_4, 25 $NaHCO_3$ and 10 D-glucose). The buffer was bubbled with 95% O_2/5% CO_2 up to pH 7.4. Slices (0.3 mm) were prepared using a Leica VT1200 vibrating blade microtome (Leica, Wetzlar, Germany) in KRB at 4 °C, and one slice per tube was allowed to recover for 30 min in KRB at 37 °C. Control hippocampal slices were incubated until the end of the experiment (15 min plus 2 h) in oxygenated KRB. OGD was induced by incubating the slices for a 15 min period in an OGD buffer in Hank's balanced salt solution (HBSS; composition in mM: 1.3 $CaCl_2$, 137 NaCl, 5 KCl, 0.65 $MgSO_4$, 0.3 Na_2HPO_4, 1.1 KH_2PO_4, and 5 HEPES), where 10 mM D-glucose was replaced by 10 mM 2-deoxy-glucose and equilibrated with a 95% N_2/5% CO_2 gas mixture, as described previously [5] After 15 min of OGD the media of the slices was replaced by oxygenated KRB and maintained for 2 h for evaluation of cellular viability and ROS generation. Guanosine (100 μM), when present, was added 15 min before (in KRB) and during OGD (in OGD buffer), and maintained in the re-oxygenation period (2 h), when the OGD buffer was replaced by physiological KRB.

2.4. Cellular Viability Evaluation

For cellular viability assessment, slices were incubated in 0.5 mg/mL 3-(4,5-dimethylthiazol-2-yl)-2,5-diphenyltetrazolium bromide (MTT) (Sigma-Aldrich) for 20 min at 37 °C, as previously described [22]. In brief, the tetrazolium ring of MTT is first cleaved by active dehydrogenases to produce a precipitated formazan. Then, precipitated formazan can be solubilized with 200 μL of dimethyl sulfoxide (DMSO) and cellular viability quantified spectrophotometrically at a wavelength of 550 nm by means of a POLARstarplate-reader (BMG Labtech, Durham, NC, USA).

2.5. Measurement of ROS Production

For evaluating ROS generation, slices were incubated with 80 μM 2′,7′-dichlorofluorescein diacetate (DCFH-DA; Sigma-Aldrich) for 30 min [23]. Then, subsequent to the OGD/reoxygenation protocol, slices were washed twice with KRB and maintained for 15 min before adding DCFH-DA. H_2DCFDA diffuses through the cell membrane, and it is hydrolyzed by intracellular esterases to the non-fluorescent form dichlorofluorescin (DCFH). Afterwards, DCFH can react with intracellular H_2O_2 to form dichlorofluorescein (DCF), a green fluorescent dye. Slices were then transferred to a 96-well black plate containing 200 μL of KRB, and fluorescence was read (excitation 480 nm, emission 525 nm) using a POLARStar plate reader (BMG Labtech).

2.6. Plasmid Constructs

The cDNA encoding the human A_1R tagged at its N-terminal tail with the O6-alkylguanine-DNA alkyltransferase (i.e., A_1R^{SNAP}) cloned in pRK5 vector (BD PharMingen, San Jose, CA, USA) was a gift from Prof. Jean-Philippe Pin (CNRS, Montpellier, France). Thus, to perform functional assays $A_{2A}R^{SNAP}$ [24] and A_1R^{SNAP} were used. Also, $A_{2A}R^{RLuc}$ and A_1R^{YFP} constructs [17] were used to perform classical BRET (Bioluminescence Resonance Energy Transfer) assays. Finally, to perform

NanoBRET experiments with the MRS7396 fluorescent antagonist, we created an $A_{2A}R$ NanoLuc sensor ($A_{2A}R^{NL}$). To this end, the cDNA encoding the human $A_{2A}R$ was amplified by polymerase chain reaction from the pECFP-$A_{2A}R$ vector using the primers: FA2AEco (5′-GCCG**GAATTC**CCCATCATGGGCTCC TCGGTGTAC-3′) and RA2ANot (5′-CGCG**GCGGCCGC**tcaggacactcctgctccatcctggg-3′). The amplified $A_{2A}R$ insert was then cloned into the *Eco*RI/*Not*I sites of pNLF1-secN vector (Promega, Stockholm, Sweden) containing a hemagglutinin (HA) epitope tag. All the constructs were verified by DNA sequencing.

2.7. Cell Culture and Transfection

Human embryonic kidney (HEK)-293T cells were grown in Dulbecco's modified Eagle's medium (DMEM) (Sigma-Aldrich), supplemented with 1 mM sodium pyruvate, 2 mM L-glutamine, 100 U/mL streptomycin, 100 mg/mL penicillin and 5% (*v/v*) fetal bovine serum at 37 °C and in an atmosphere of 5% CO_2. HEK-293T cells growing in 60 cm^2 plates were transfected with the cDNA encoding the different plasmids using linear PolyEthylenImine reagent (PEI) (Polysciences Inc., USA).

2.8. NanoBRET Experiments

The NanoBRET assay was performed on stably expressing ($A_{2A}R^{NL}$) HEK-293T cells, transiently transfected (or not) with A_1R^{SNAP}, according to [25]. In brief, cells were re-suspended in HBSS, and seeded into poly ornithine coated white 96-well plates. After 24 h, cells were challenged with/without the non-labelled $A_{2A}R$ antagonist (SCH442416) or guanosine and incubated for 1 h at 37 °C. Subsequently, the fluorescent ligand (MRS7396) was added and the plate and returned to 37 °C for 1 h. Finally, coelenterazine-h (Life Technologies Corp.) was added at a final concentration of 5 μM, and readings were performed after 5 min using a CLARIOStar plate reader (BMG Labtech). The donor and acceptor emissions were measured at 490–510 nm and 650–680 nm, respectively. The raw NanoBRET ratio was calculated by dividing the 650 nm emission by the 490 nm emission. In competition studies, results were expressed as a percentage of the maximum signal obtained (mBU; milliBRET Units).

2.9. cAMP Assay

cAMP accumulation was measured using the LANCE® Ultra cAMP Kit (PerkinElmer, Waltham, MA, USA) as previously described [26]. In brief, transfected ($A_{2A}R^{SNAP}$ or $A_{2A}R^{SNAP}$ + A_1R^{SNAP}) HEK-293T cells were firstly incubated for 1 h at 37 °C with stimulation buffer (BSA 0.1%, ADA 0.5 units/mL, zardaverine 2 μM; in serum-free DMEM) and later on with CGS21680 for 30 min at 37 °C. Thereafter, cells were transferred to a 384-well plate in which reagents were added following manufacturer's instructions. After 1 h at room temperature, Time-Resolved-Fluorescence Resonance Energy Transfer (TR-FRET) was determined by measuring light emission at 620 nm and 665 nm by means of a CLARIOstar plate reader (BMG Labtech).

2.10. Intracellular Calcium Determinations

The A_1R-mediated intracellular Ca^{2+} accumulation was assessed by means of a luciferase reporter assay based on the expression of the nuclear factor of activated T-cells (NFAT), as previously described [27]. In brief, cells were transfected with the cDNA encoding the A_1R, the NFAT-luciferase reporter (pGL4-NFAT-RE/luc2p; Promega) and the yellow fluorescent protein (pEYFP-N1; Promega). After 36 h post-transfection, cells were incubated with the indicated drugs for 6 h. Subsequently, cells were harvested with passive lysis buffer (Promega), and the luciferase activity of cell extracts was determined using a luciferase Bright-Glo^{TM} assay (Promega) in a POLARStar plate-reader (BMG Labtech) using a 30-nm bandwidth excitation filter at 535 nm.

2.11. Label-Free Cellular Impedance Assay

The xCELLigence Real-Time Cell Analyzer (RTCA) system (ACEA Biosciences, San Diego, CA, USA) was employed to measure changes in cellular impedance correlating with cell spreading and tightness, thus being widely accepted as a morphological and functional biosensor of cell status [28–30]. Thus, 16-well E-plates (ACEA Biosciences) were coated with 50 μL fibronectin (10 μg/mL) at 37 °C for 1 h before being washed three times with 100 μL MilliQ-water before use. The background index for each well was determined with 90 μL of stimulation buffer (supplemented DMEM with ADA 0.5 U/mL and zardaverine 10 μM) in the absence of cells. Data from each well were normalized to the time point just before compound addition using the RTCA software providing the normalized cell index (NCI). Subsequently, HEK-293T cells permanently expressing the $A_{2A}R^{SNAP}$ construct [31] in the absence or presence of A_1R^{SNAP} (90 μL resuspended in stimulation buffer) were then plated at a cell density of 40,000 cells/well and grown for 18 h in the RTCA SP device station (ACEA Biosciences) at 37 °C and in an atmosphere of 5% CO_2 before ligand (i.e., CGS21680 and/or guanosine) addition. Cell index values were obtained immediately following ligand stimulation every 15 s for a total time of at least 50 min. For data analysis, the area under the curve (AUC) for each NCI trace response was quantified and normalized to the basal.

2.12. Statistics

Data are represented as mean ± standard error of mean (SEM). The number of samples/animals (*n*) in each experimental condition is indicated in the corresponding figure legend. Comparisons among experimental groups were performed by Student's *t*-test and ANOVA, using GraphPad Prism 6.01 (San Diego, CA, USA), as indicated. Statistical difference was accepted when $p < 0.05$.

3. Results

3.1. Guanosine-Mediated Neuroprotection in Hippocampal Slices Depends on $A_{2A}R$ Expression

It has been postulated that ARs might be involved in guanosine-mediated responses in vivo [16]. Within this line of inquiry, we first interrogated whether $A_{2A}R$ expression is necessary for guanosine-mediated neuroprotection, a well-known guanosine effect in vivo [1]. To this end, we subjected hippocampal slices from wild-type (i.e., $A_{2A}R^{+/+}$) and $A_{2A}R^{-/-}$ mice to an OGD protocol in the presence or absence of guanosine. Indeed, significant cell death ($p < 0.001$) and ROS production ($p = 0.0359$) were observed in $A_{2A}R^{+/+}$ hippocampal slices subjected to the OGD protocol (Figure 1A,B). Interestingly, guanosine (100 μM) was able to prevent these effects, thus cellular viability significantly increased ($p = 0.0012$) and ROS production decreased ($p = 0.0389$) (Figure 1A,B), as previously reported [5,11]. Importantly, under the same experimental conditions, in hippocampal slices obtained from $A_{2A}R^{-/-}$ mice, guanosine failed to prevent OGD-mediated cell death ($p = 0.005$) and ROS production ($p = 0.0279$) (Figure 1A,B), thus losing its neuroprotective effect. Overall, these results suggested that $A_{2A}R$ expression was necessary for guanosine-mediated neuroprotection.
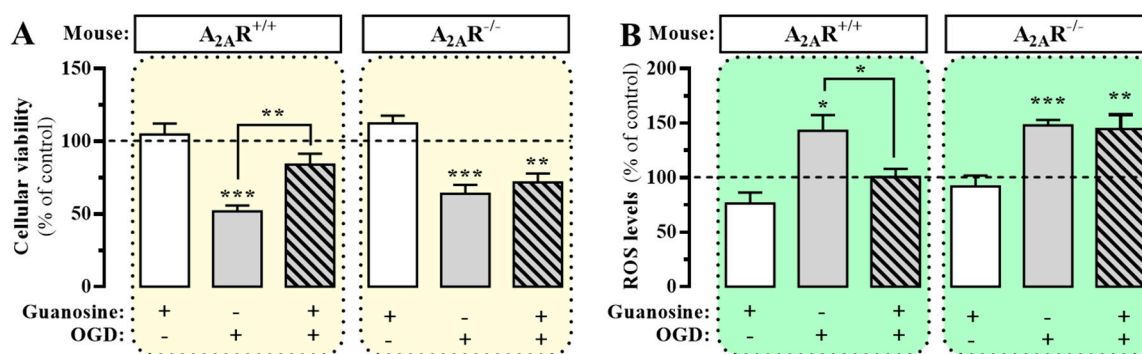
Figure 1. Guanosine-mediated neuroprotection in mouse hippocampal slices. Hippocampal slices from $A_{2A}R^{+/+}$ and $A_{2A}R^{-/-}$ mice were subjected to oxygen/glucose deprivation (OGD) in the absence or presence of guanosine (100 µM) for 15 min before, and during OGD and re-oxygenation. The cellular viability (**A**) was assessed by MTT reduction whereas ROS levels (**B**) were measured after incorporation of the DCFDA fluorescent probe. Results were normalized to the control slices (vehicle-treated slices, dashed line) and expressed as mean ± SEM of three independent experiments performed in triplicate. The asterisks indicate statistically significant differences (* $p <0.05$, ** $p < 0.01$ and *** $p < 0.001$; one-way ANOVA with Tukey's post-hoc test).

3.2. $A_{2A}R$ Ligand Binding is Affected by Guanosine upon A_1R Coexpression

Once we demonstrated that the neuroprotective effect of guanosine was $A_{2A}R$-dependent, we aimed to assess the putative direct interaction of guanosine with $A_{2A}R$ through ligand binding studies. To this end, we engineered a fluorescent ligand BRET-based assay to assess $A_{2A}R$ ligand binding in living cells (Figure 2A). We used a fluorescent $A_{2A}R$ antagonist (MRS7396) that is able to engage in a BRET process upon interacting with a cell surface $A_{2A}R$ tagged with the NanoLuciferase (NL) at its N-terminus (i.e., $A_{2A}R^{NL}$) (Figure 2A). MRS7396 is a BODIPY630/650 derivative of SCH442416 [19], which upon $A_{2A}R$ binding can act as an acceptor chromophore for NanoLuciferase emission (490 nm) in a BRET process. Thus, we challenged stable $A_{2A}R^{NL}$-expressing cells with increasing concentrations of MRS7396, in the presence/absence of non-labelled SCH442416. Interestingly, a bell-shaped binding saturation hyperbola, with a $K_D = 4.8 \pm 2.7$ nM, was obtained for MRS7396, while in the presence of a saturating concentration of SCH442416 (1 µM) the binding was displaced (Figure 2B). Our results showed that the NanoBRET binding assay was a robust and reliable way to assess $A_{2A}R$ ligand binding. Accordingly, we next assessed possible guanosine effects on $A_{2A}R$ orthosteric binding by performing a competition assay with a fixed concentration of MRS7396 (10 nM) (occupying ~80% of receptors at equilibrium) and increasing concentrations of guanosine. Interestingly, under these experimental conditions, guanosine was unable to alter MRS7396 binding to $A_{2A}R^{NL}$ (Figure 2C), thus indicating that guanosine does not orthosterically bind to $A_{2A}R$, as previously reported [12,13].

Since $A_{2A}R$ heteromerizes with A_1R [17], and some of the physiological effects of guanosine were modulated by A_1R ligands [32,33], we investigated whether $A_1R/A_{2A}R$ heteromer formation affected AR-related guanosine-dependent effects. To this end, we first recreated the formation of $A_1R/A_{2A}R$ heteromers in HEK-293T cells by transfecting $A_{2A}R^{RLuc}$ and A_1R^{YFP} constructs and monitoring $A_{2A}R/A_1R$ heteromerization by a classical BRET approach (Figure A1). Interestingly, neither adenosine nor guanosine incubation altered $A_1R/A_{2A}R$ heteromer formation (Figure A1). Subsequently, we assessed the impact of A_1R co-expression in $A_{2A}R$ binding of MRS7396 using our NanoBRET binding assay. Notably, in A_1R-$A_{2A}R$ doubly expressing cells, guanosine (100 µM) was able to significantly reduce by $19 \pm 4\%$ ($p = 0.0138$) the binding of MRS7396 to the $A_{2A}R^{NL}$, thus indicating that the $A_1R/A_{2A}R$ heteromer might play a potential role in AR-related guanosine-dependent effects (Figure 2C).
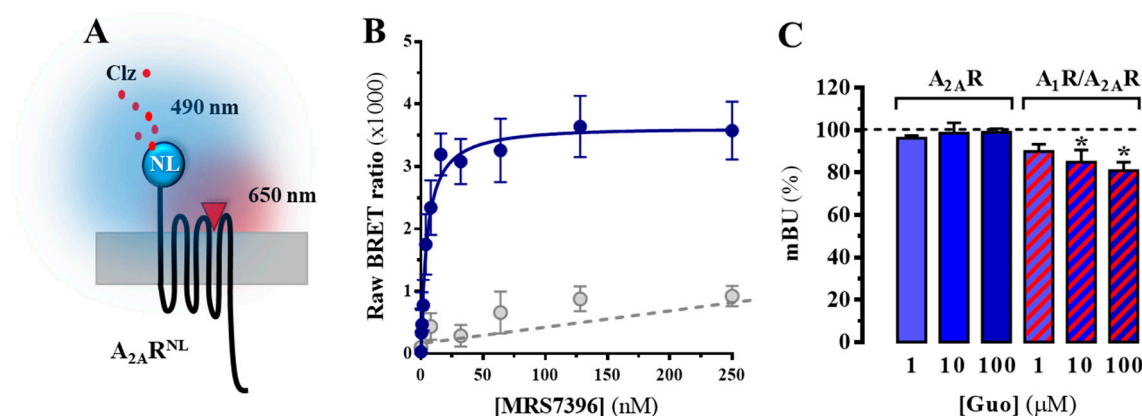
Figure 2. NanoBRET-based $A_{2A}R$ binding determinations. (**A**) Schematic representation of the NanoBRET-based assay using $A_{2A}R^{NL}$ stably expressing cells and the fluorescent MRS7396 ligand (red triangle). When the coelenterazine (Clz) substrate is metabolized by NanoLuciferase (NL), its 475 nm light emission may engage in a BRET process with MRS7396 given the close proximity (i.e., bound to $A_{2A}R^{NL}$). (**B**) NanoBRET signal for $A_{2A}R^{NL}$ with increasing MRS7396 concentrations in the absence (solid line) and presence (dotted line) of 1 μM SCH442416. (**C**) Guanosine (Guo) effects on MRS7396 binding to cells expressing $A_{2A}R^{NL}$ (blue bars) or $A_{2A}R^{NL}$ plus A_1R^{SNAP} (red dashed bars). Cells were incubated with MRS7396 (10 nM) and increasing guanosine concentrations (1–100 μM) in the presence or absence of 1 μMSCH442416 to allow specific binding calculations. Results were normalized to the MRS7396 specific binding in the absence of guanosine for each transfection set and expressed as mean ± SEM of four independent experiments performed in triplicate. The asterisks indicate statistically significant differences * $p < 0.05$, one-way ANOVA followed by Dunnett's post-hoc testwhile compared to control (dashed line).

3.3. $A_{2A}R$ Signalling, but Not A_1R, is Modulated by Guanosine in an A_1R Coexpression-Dependent Manner

Given that guanosine reduced $A_{2A}R$ binding in an A_1R-expression-dependent manner, we next aimed to determine whether guanosine also impinged into $A_{2A}R$ signaling. Accordingly, we determined the effects of guanosine in $A_{2A}R$-mediated cAMP accumulation upon agonist incubation. In $A_{2A}R$-expressing cells, the selective $A_{2A}R$ full agonist CGS21680 induced a concentration-dependent cAMP accumulation ($pEC_{50} = 7.98 \pm 0.08$), indicating that the receptor was expressed and functional at the plasma membrane (Figure 3A). Subsequently, we challenged cells with a fixed concentration of CGS21680 (200 nM) and evaluated the effects of increasing concentrations of guanosine in $A_{2A}R$-dependent cAMP accumulation. As shown in Figure 3B, guanosine did not preclude $A_{2A}R$-mediated cAMP accumulation. Conversely, in cells doubly expressing A_1R and $A_{2A}R$, guanosine (100 μM) was able to significantly reduce, by $19 \pm 3\%$ ($p = 0.0460$), the $A_{2A}R$-mediated cAMP accumulation (Figure 3B). These results supported the hypothesis that the effects of guanosine might be dependent on an A_1R-$A_{2A}R$ interaction.

Interestingly, our NanoBRET-based binding results and cAMP determinations in the absence and presence of A_1R suggested a direct involvement of this receptor in guanosine-mediated blockade of $A_{2A}R$ ligand binding and signaling. Thus, to ascertain whether guanosine would directly interact with A_1R we assessed its impact on A_1R-dependent signaling. To this end, A_1R-mediated calcium responses in HEK-293T cells were determined through a homogenous bioluminescence reporter assay system using a NFAT response element controlling luciferase gene expression. While the activation of A_1R, via application of the agonist N^6-R-phenylisopropyladenosine (R-PIA, 50 nM), increased intracellular Ca^{2+}, the incubation with guanosine (100 μM) did not promote intracellular Ca^{2+} mobilization (Figure 4A). Similarly, when A_1R-expressing cells were treated with R-PIA in the presence of increasing concentrations of guanosine, A_1R-dependent intracellular Ca^{2+} mobilization was not affected, as observed in doubly A_1R and $A_{2A}R$ transfected cells (Figure 4B). Overall, these results

indicated that guanosine did not interact with A_1R, thus ruling out any orthosteric A_1R-dependent trans-inhibition of $A_{2A}R$ function in A_1R-$A_{2A}R$ expressing cells.
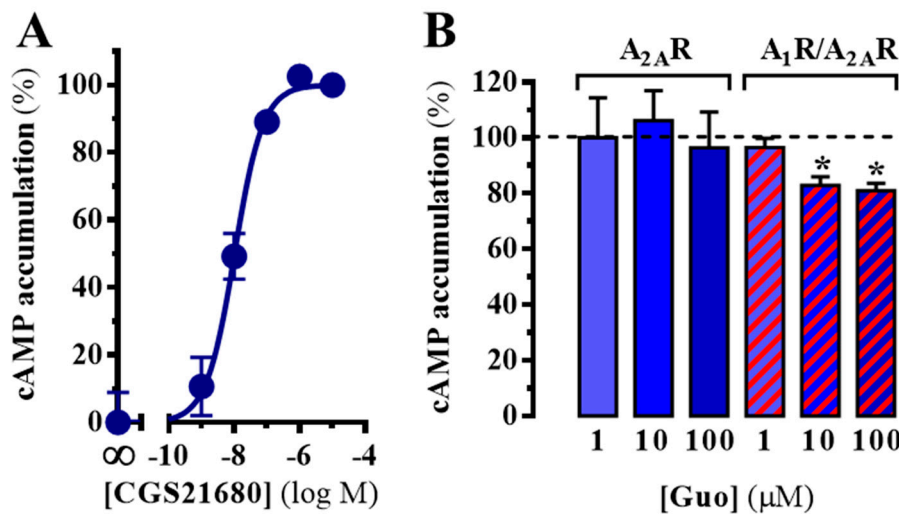

Figure 3. $A_{2A}R$-dependent cAMP accumulation. (**A**) Concentration-dependent effects of CGS21680 in cAMP accumulation in singly $A_{2A}R$ expressing cells. The signal was normalized by assigning the 100% to the maximum signal obtained and 0% to cells without ligand. The data are expressed as the mean ± SD of a representative experiment performed in triplicate. (**B**) Guanosine effects on CGS21680-mediated cAMP accumulation in cells expressing $A_{2A}R^{SNAP}$ (blue bars) or $A_{2A}R^{SNAP}$ plus A_1R^{SNAP} (red dashed bars). Results were normalized to the specific cAMP accumulation in the absence of guanosine for each transfection set and are expressed as mean ± SEM of four independent experiments performed in triplicate. The asterisks indicate statistically significant differences * $p < 0.05$, one-way ANOVA followed by Dunnett's post-hoc testwhile compared to control (dashed line).

Finally, we assessed the functional activity of guanosine using the label-free technology. To this end, the whole-cell guanosine-mediated impedance responses were monitored in living cells expressing $A_{2A}R$ in the absence or presence of A_1R using a biosensor method, as previously reported [34]. First, we tested CGS21680-mediated changes in morphology (i.e., impedance) of $A_{2A}R^{SNAP}$ expressing HEK-293T cells, which were recorded in real-time. Interestingly, addition of CGS21680 resulted in a significant ($p = 0.015$) increase of impedance, which was blocked by incubation with the selective $A_{2A}R$ antagonist ZM241385 (Figure 5A,B). In addition, guanosine did not affect the cell basal morphology ($p = 0.6105$) nor its CGS218680-mediated changes ($p = 0.1217$) (Figure 5B). However, in doubly expressing $A_1R/A_{2A}R$ cells guanosine significantly reduced ($p < 0.0106$) cell basal morphology and precluded ($p < 0.0001$) the CGS218680-induced increase in cellular impedance (Figure 5B). Again, these results indicated that the A_1R-$A_{2A}R$ co-expression may play a potential role in AR-related guanosine-dependent cellular effects.
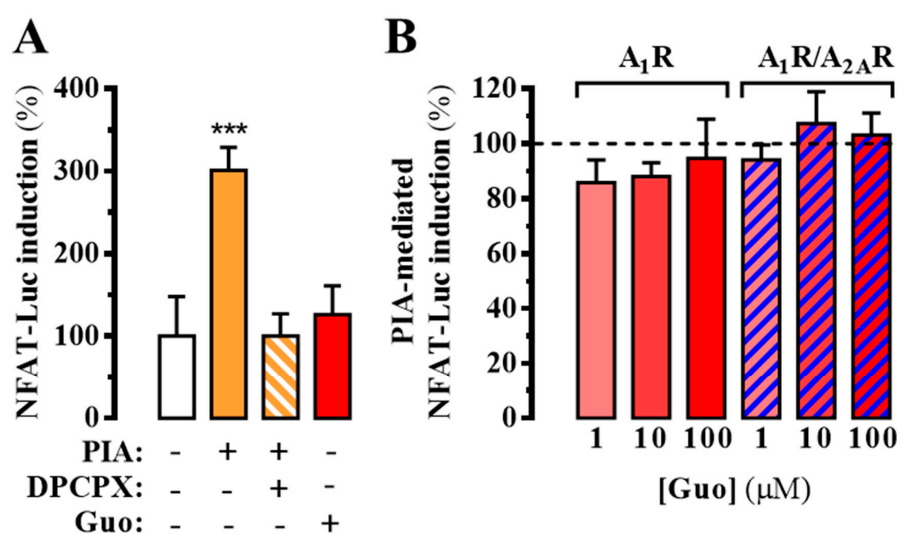
Figure 4. A_1R-dependent intracellular Ca^{2+} mobilization. (**A**) Determination of A_1R-mediated intracellular calcium accumulation by means of a luciferase reporter assay system. HEK-293T cells were transiently transfected with the firefly luciferase-encoding plasmid (pGL4-NFAT-luc2p) and the cDNAs encoding the A_1R^{SNAP} and the YFP. Thirty-six hours after transfection, cells were treated 6 h with the A_1R agonist R-PIA (PIA, 50 nM) in the absence or presence of DPCPX (500 nM) or guanosine (Guo, 100 µM). Light emission is presented as the percentage increase over basal levels. The data are expressed as the mean ± SEM of three independent experiments performed in triplicate. The asterisks indicate statistically significant differences *** $p < 0.001$, one-way ANOVA followed by Dunnett's post-hoc test when compared to control. (**B**) Guanosine modulation of R-PIA-mediated intracellular Ca^{2+} mobilization (PIA-mediated NFAT-Luc induction) in cells expressing A_1R^{SNAP} (red bars) or A_1R^{SNAP} plus $A_{2A}R^{SNAP}$ (blue dashed bars). The dotted line represents the Ca^{2+} mobilization induced by R-PIA in the absence of guanosine within each cell transfection group. The data are expressed as the mean ± SEM of three independent experiments performed in triplicate.
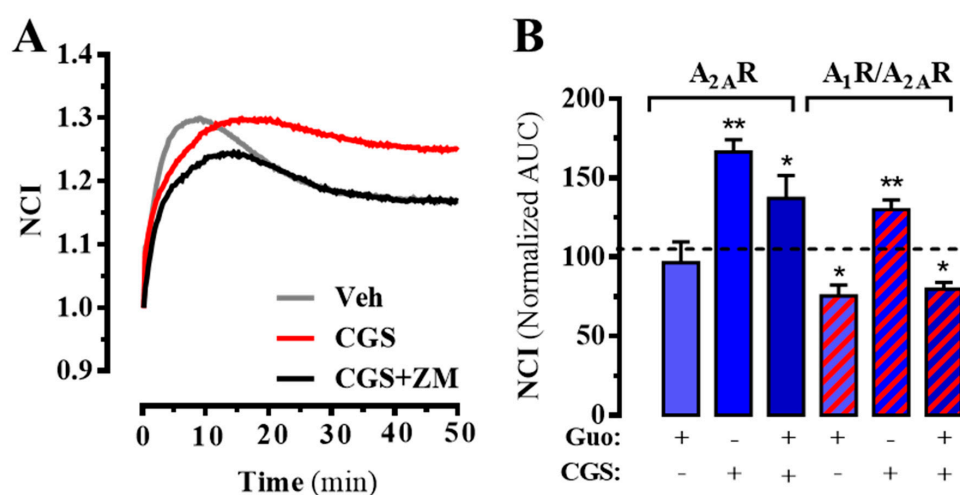

Figure 5. $A_{2A}R$-mediated whole-cell label-free responses. (**A**) Real-time cellular impedance changes upon CGS21680 (200 nM) incubation in the absence or presence of ZM241385 (1 µM). The signal was normalized when the ligand was added. (**B**) Guanosine (100 µM) effects on CGS21680-mediated cellular impedance changes in cells expressing $A_{2A}R^{SNAP}$ (blue bars) or $A_{2A}R^{SNAP}$ plus A_1R^{SNAP} (dashed red bars). Results are presented as area under the cure (AUC) and normalized to the AUC in the basal condition (i.e., absence of any drug) for each transfection set and expressed as mean ± SEM of three independent experiments performed in duplicate. * $p < 0.05$ and ** $p < 0.01$, one-way ANOVA followed by Dunnett's post-hoc test while compared to control (dashed line).

4. Discussion

Guanosine is a purine nucleoside with widely demonstrated extracellular neuromodulatory effects in the CNS, but so far without an identified receptor. Based on the use of selective ligands, ARs have been proposed as possible targets to explain guanosine-mediated effects in animal and cellular models of ischemia. However, at present, the mechanism of action of guanosine is not clear. Here, we show that $A_{2A}R$ expression was crucial for guanosine-mediated protective effects in an ex vivo model of brain ischemia. In addition, when examining guanosine effects in a controlled heterologous system, we were able to reveal the importance of a proposed A_1R-$A_{2A}R$ interaction mediating guanosine effects, both in $A_{2A}R$-ligand binding and in receptor function.

In the OGD ischemia model in hippocampal slices, we previously showed that guanosine induced a neuroprotective effect (increase of glutamate uptake) that was inhibited by activation of $A_{2A}R$ by CGS2180 [11]. This effect of CGS21680 in abolishing a guanosine-evoked increase in glutamate uptake in an OGD protocol was also observed in cultured astrocytes expressing the astrocytic glutamate transporter Glt-1 [15]. Therefore, here we evaluated guanosine's neuroprotective effects in $A_{2A}R^{-/-}$ mice and revealed an important role for this receptor. Thus, in $A_{2A}R^{-/-}$ hippocampal slices, we observed a loss of the neuroprotective effects of guanosine (increasing viability and controlling ROS production in OGD conditions) that were observed in slices from wild-type mice (Figure 6A). This result, consistent with previous data, pointed to ARs as possible targets for guanosine [35,36], prompting us to further explore the mechanism by which guanosine might act.
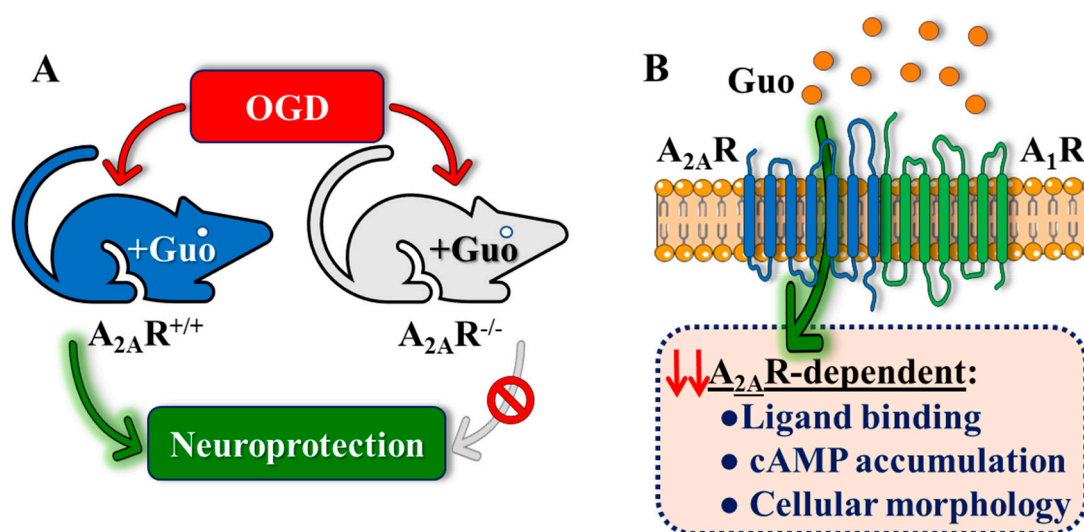

Figure 6. Schematic summary of the overall findings. (**A**) Guanosine-mediated neuroprotection in mouse is dependent on $A_{2A}R$ expression. Thus, guanosine fails to neuroprotect from OGD damage in $A_{2A}R^{-/-}$ mouse hippocampal slices. (**B**) Guanosine modulates $A_{2A}R$ functionality in living cells in an A_1R-dependent manner. While guanosine does not interfere with A_1R-dependent signaling, it modulates $A_{2A}R$ binding and intracellular signaling (i.e., cAMP accumulation and cellular morphology) only in A_1R-$A_{2A}R$ co-expressing cells. Therefore, A_1R and $A_{2A}R$ may constitute a molecular substrate involved in guanosine-mediated effects, but the precise mechanism of action of guanosine involving ARs is still lacking.

Our NanoBRET-based sensor data suggested that, as previously reported [13], guanosine apparently does not bind directly to the $A_{2A}R$. However, in $A_1R/A_{2A}R$ cells, it was possible to observe a guanosine-mediated partial displacement of $A_{2A}R$-ligand binding (Figure 6B). Together with the ex vivo data, this result would indicate that the mechanism of action of guanosine would be mediated by this receptor–receptor entity. Indeed, previous data showing both DPCPX- and pertussis toxin-dependent blockade of protective effects of guanosine in hippocampal slices subjected

to OGD [11], supported the dependence on functional A_1Rs coupled to a G-protein to mediate guanosine effects.

We found that guanosine reduced $A_{2A}R$ orthosteric binding only in A_1R-$A_{2A}R$ expressing cells. Thus, we evaluated whether guanosine could modulate $A_{2A}R$-dependent signaling under the same experimental conditions. Interestingly, while guanosine did not preclude CGS21680-induced cAMP accumulation in $A_{2A}R$-expressing cells, it reduced $A_{2A}R$-mediated cAMP accumulation in doubly A_1R-$A_{2A}R$ transfected cells, as observed in the ligand-binding assay (Figure 6B). Additionally, the evaluation of guanosine effects on the functional activity of ARs using the label-free technology confirmed that guanosine-mediated cell impedance responses were dependent on A_1R-$A_{2A}R$ co-expression. Hence, our results indicate that guanosine could attenuate $A_{2A}R$ signaling (i.e., agonist-mediated cAMP accumulation and cell impedance responses) in an A_1R-dependent manner (Figure 6B). On the other hand, when the A_1R-dependent signaling (i.e., intracellular Ca^{2+} mobilization) was assessed, guanosine was unable to modulate receptor's function both in singly and doubly A_1R-$A_{2A}R$ transfected cells. Taken together, our results suggest that while guanosine did not signal through A_1R, it requires this receptor to exert its $A_{2A}R$ modulatory effect, which could indicate that the $A_1R/A_{2A}R$ heteromer might be a molecular substrate for guanosine.

The $A_1R/A_{2A}R$ heteromer displays some functional characteristics similar to that reported for other AR-containing oligomers, for instance $A_{2A}R$ combined with the dopamine D_2 receptor (D_2R) or the cannabinoid CB_1 receptor (CB_1R) [37]. Interestingly, these receptor heteromers have been shown to exert reciprocal receptor-receptor allosteric antagonistic interactions [38]. Precisely, an $A_1R/A_{2A}R$ heteromer-mediated transmembrane-dependent negative allosteric interaction at the ligand-receptor binding level has been described [39]. In addition, co-activation of both receptors led to a canonical protein Gs-Gi antagonistic interaction at the level of the adenylyl cyclase [40]. This situation makes it difficult to conclude whether an effect in a given signaling pathway is caused by either the allosteric or the canonical interaction. Thus, our data showing that guanosine was able to modulate AR functioning (i.e., cAMP assay) only in cells expressing A_1R and $A_{2A}R$ do not permit a clear determination of the interaction at the intracellular level (i.e., canonical protein Gs-Gi antagonistic interaction). However, considering the whole picture, it seems likely that guanosine effects in the physiological context may depend on the co-expression of both receptors and their and interaction. Indeed, guanosine did not disrupt the $A_1R/A_{2A}R$ heteromer, as observed by a saturable BRET signal, similar to that obtained following adenosine treatment, and by membrane co-localization of A_1R and $A_{2A}R$ in guanosine-treated cells (Figure A1).

Overall, our data suggest an important role for the A_1-A_{2A} receptor–receptor interaction in guanosine-mediated effects. Thus, while our results seem to rule out an eventual guanosine-mediated A_1R-$A_{2A}R$ canonical antagonistic interaction, further investigation is needed to ascertain whether guanosine may either modulate the well-known A_1R-$A_{2A}R$ allosteric interaction or an indirect mechanism of action yet to be discovered.

5. Conclusions

In summary, our results revealed that certain AR-related guanosine-mediated effects rely on A_1R and $A_{2A}R$ co-expression. Indeed, in ex vivo experiments, the well-known guanosine-mediated neuroprotective effect depends on $A_{2A}R$ expression. Thus, guanosine failed to protect $A_{2A}R^{-/-}$ mouse hippocampal slices from ischemia-induced damage. In addition, while guanosine did not interfere with A_1R-mediated signaling, it modulated $A_{2A}R$ binding and intracellular signaling only in A_1R-$A_{2A}R$ co-expressing cells. Overall, our results suggest that A_1R and $A_{2A}R$ may constitute a molecular substrate involved in guanosine effects, but the precise mechanism of action of guanosine involving ARs still is intriguing.

Author Contributions: D.L., C.M.M., V.M. and T.Š. performed experiments and analyzed results. R.D. and K.A.J. synthesized the fluorescent ligand and analyzed results. V.F.-D. performed experiments, analyzed results and

wrote the paper. C.I.T. and F.C. conceived the project, analyzed results and wrote the paper. All authors read and approved the final manuscript.

Conflicts of Interest: The authors declare no conflict of interest. The funders had no role in the design of the study; in the collection, analyses, or interpretation of data; in the writing of the manuscript; or in the decision to publish the results.

Appendix A

Appendix A.1 Materials and Methods

Appendix A.1.1 Immunocytochemistry

Transfected HEK-293T cells growing on coverslips were fixed in 4% paraformaldehyde for 15 min and exposed to goat anti-$A_{2A}R$ antibody (1 μg/mL; Santa Cruz Biotechnology Inc., Dallas, TX, USA) plus a rabbit anti-A_1R antibody (1 μg/mL; Millipore, Billerica, MA, USA). Primary antibodies were detected using a Cy3-conjugated donkey anti-goat antibody (1/200; Jackson ImmunoResearch Laboratories Inc., West Grove, PA, USA) and Cy2-conjugated donkey anti-rabbit antibody (1/200; Jackson ImmunoResearch Laboratories Inc.). Coverslips were rinsed for 30 min, mounted with Vectashield immunofluorescence medium (Vector Laboratories, Peterborough, UK) and examined using a Leica TCS 4D confocal scanning laser microscope (Leica Lasertechnik GmbH, Heidelberg, Germany).

Appendix A.1.2 BRET

BRET saturation experiments were performed as previously described [41]. In brief, HEK-293T cells were transiently transfected with a constant amount of the $A_{2A}R^{Rluc}$ and increasing amounts of A_1R^{YFP}. After 48 h, cells were rapidly washed twice in PBS, detached and resuspended in Hank's balanced salt solution buffer (137 mM NaCl, 5.4 mM KCl, 0.25 mM Na_2HPO_4, 0.44 mM KH_2PO_4, 1.3 mM $CaCl_2$, 1.0 mM $MgSO_4$, 4.2 mM $NaHCO_3$, pH 7.4), containing 10 mM glucose. Cell suspensions were distributed in triplicate into 96-well microplate black plates (Corning, Stockholm, Sweden) for fluorescence measurement or white plates (Corning 3600) for BRET determination. For BRET measurement, 5 μM benzyl-coelenterazine (NanoLight Technology, Prolume Ltd., Pinetop, AZ, USA) was added, and readings were performed 1 min after substrate addition using the POLARstar Omega plate-reader (BMG Labtech, Durham,NC, USA), which allows the simultaneous integration of the signals detected with two filter settings [485 nm (440–500 nm) and 530 nm (510–560 nm)]. The BRET ratio was defined and represented as previously described [41].

Appendix A.2 Results

We aimed to assess whether guanosine treatment modulated the $A_1R/A_{2A}R$ heteromerization status. To this end, we performed immunocytochemistry analyses and constructed classical A_1R-$A_{2A}R$ heteromer-based BRET saturation curves (Figure A1). Our immunocytochemistry experiments revealed that $A_{2A}R$ and A_1R co-distributed in transiently transfected HEK-293T cell, as previously reported [17], and that 2 h incubation with guanosine did not alter their apparent co-distribution (Figure A1A). Subsequently, the close proximity of the two receptors was monitored through BRET saturation analysis in cells transiently expressing $A_{2A}R^{Rluc}$ and increasing concentrations of A_1R^{YFP} showing a

bell-shaped BRET saturation curve ($\text{BRET}_{50} = 0.38 \pm 0.07$ and $\text{BRET}_{max} = 90 \pm 6$), thus indicating the formation of constitutive A_1R-$A_{2A}R$ complexes in living cells (Figure A1B). Importantly, under the same experimental conditions, the treatment with either adenosine (100 µM) or guanosine (100 µM) for 2 h did not alter the physical proximity of A_1R and $A_{2A}R$. Thus, neither the BRET_{50} [$F_{(2,30)} = 1.524$, *p*-value = 0.2343] nor the BRET_{max} [$F_{(2,30)} = 0.3135$, *p*-value = 0.7333] was significantly affected by adenosine or guanosine incubation (Figure A1B). Overall, these results corroborated the formation of $A_1R/A_{2A}R$ heterocomplexes in living cells, as previously described [17], and that these complexes were not affected by adenosine or guanosine, consistent with the general notion that GPCR homo- and heteromerization is often constitutive.
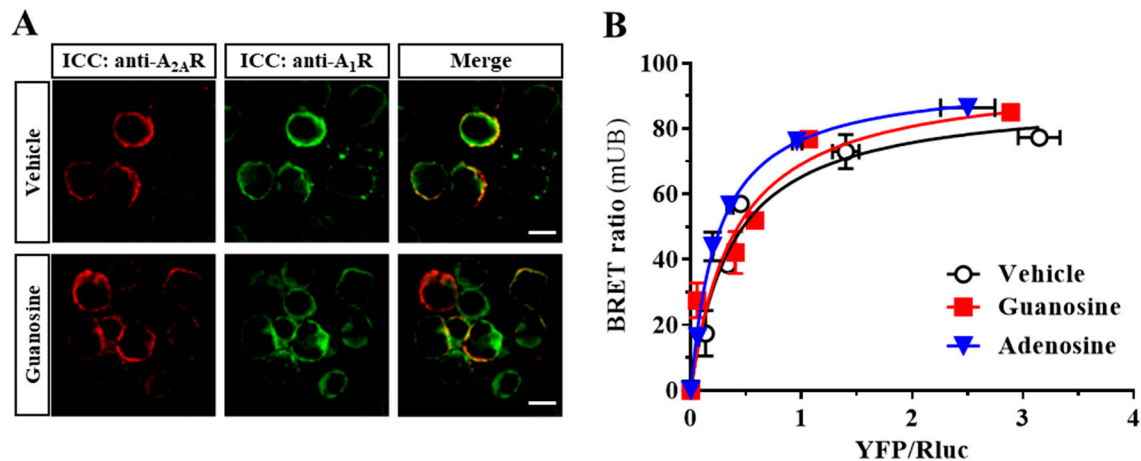

Figure A1. A_1R and $A_{2A}R$ interaction in HEK-293T cells. (**A**) Co-distribution of $A_{2A}R$ and A_1R in HEK-293T. Cells transiently transfected with $A_{2A}R^{SNAP}$ and A_1R^{SNAP} and incubated with vehicle or guanosine (100 µM) for 2 h. Cells were processed for immunocytochemical (ICC) detection of $A_{2A}R$ (red) and A_1R (green) using specific antibodies (see Appendix A.1). Merged images reveal co-distribution of $A_{2A}R^{SNAP}$ and A_1R^{SNAP} (yellow). Scale bar: 100 µm. (**B**) BRET saturation curve between $A_{2A}R$ and A_1R. BRET was measured in HEK-293T cells co-expressing $A_{2A}R^{Rluc}$ and A_1R^{YFP} constructs and incubated with vehicle, adenosine (100 µM) or guanosine (100 µM) for 2 h. Cells were co-transfected with a fixed amount of $A_{2A}R^{Rluc}$ and increasing amounts A_1R^{YFP}. Plotted on the *X*-axis is the fluorescence value obtained from the YFP, normalized with the luminescence value of the *R*luc constructs 10 min after coelenterazine h incubation and in the *Y*-axis the corresponding BRET ratio (×1000). mBU: mBRET units. Results are expressed as mean ± SEM of four independent experiments grouped as a function of the amount of acceptor fluorescence.

References

1. Lanznaster, D.; Dal-Cim, T.; Piermartiri, T.C.B.; Tasca, C.I. Guanosine: A Neuromodulator with Therapeutic Potential in Brain Disorders. *Aging Dis.* **2016**, *7*, 657–679. [CrossRef] [PubMed]

2. Di Liberto, V.; Mudò, G.; Garozzo, R.; Frinchi, M.; Fernandez-Dueñas, V.; Di Iorio, P.; Ciccarelli, R.; Caciagli, F.; Condorelli, D.F.; Ciruela, F.; et al. The guanine-based purinergic system: The tale of an orphan neuromodulation. *Front. Pharmacol.* **2016**, *7*, 158. [CrossRef] [PubMed]

3. Durukan, A.; Tatlisumak, T. Acute ischemic stroke: Overview of major experimental rodent models, pathophysiology, and therapy of focal cerebral ischemia. *Pharmacol. Biochem. Behav.* **2007**, *87*, 179–197. [CrossRef] [PubMed]

4. Candelario-Jalil, E. Injury and repair mechanisms in ischemic stroke: Considerations for the development of novel neurotherapeutics. *Current Opin. Investig. Drugs (Lond. Engl. 2000)* **2009**, *10*, 644–654.

5. Dal-Cim, T.; Martins, W.C.; Santos, A.R.S.; Tasca, C.I. Guanosine is neuroprotective against oxygen/glucose deprivation in hippocampal slices via large conductance Ca^{2+}-activated K+ channels, phosphatidilinositol-3 kinase/protein kinase B pathway activation and glutamate uptake. *Neuroscience* **2011**, *183*, 212–220. [CrossRef] [PubMed]

6.   Dal-Cim, T.; Molz, S.; Egea, J.; Parada, E.; Romero, A.; Budni, J.; Martín de Saavedra, M.D.; del Barrio, L.; Tasca, C.I.; López, M.G. Guanosine protects human neuroblastoma SH-SY5Y cells against mitochondrial oxidative stress by inducing heme oxigenase-1 via PI3K/Akt/GSK-3β pathway. *Neurochem. Int.* **2012**, *61*, 397–404. [CrossRef]

7.   Ganzella, M.; de Oliveira, E.D.A.; Comassetto, D.D.; Cechetti, F.; Cereser, V.H.; Moreira, J.D.; Hansel, G.; Almeida, R.F.; Ramos, D.B.; Figueredo, Y.N.; et al. Effects of chronic guanosine treatment on hippocampal damage and cognitive impairment of rats submitted to chronic cerebral hypoperfusion. *Neurol. Sci.* **2012**, *33*, 985–997. [CrossRef]

8.   Tasca, C.; Llorente, J.; Dal-Cim, T.; Fernandez-Duenas, V.; Gomez-Soler, M.; Gandia, J.; Ciruela, F. The neuroprotective agent Guanosine activates big conductance Ca2+-activated Potassium channels (BK) transfected to HEK-293 cells. *J. Neurochem.* **2013**, *125*, 273.

9.   Hansel, G.; Tonon, A.C.; Guella, F.L.; Pettenuzzo, L.F.; Duarte, T.; Duarte, M.M.M.F.; Oses, J.P.; Achaval, M.; Souza, D.O. Guanosine Protects Against Cortical Focal Ischemia. Involvement of Inflammatory Response. *Mol. Neurobiol.* **2015**, *52*, 1791–1803. [CrossRef]

10.   Dal-Cim, T.; Martins, W.C.; Thomaz, D.T.; Coelho, V.; Poluceno, G.G.; Lanznaster, D.; Vandresen-Filho, S.; Tasca, C.I. Neuroprotection Promoted by Guanosine Depends on Glutamine Synthetase and Glutamate Transporters Activity in Hippocampal Slices Subjected to Oxygen/Glucose Deprivation. *Neurotox. Res.* **2016**, *29*, 460–468. [CrossRef]

11.   Dal-Cim, T.; Ludka, F.K.; Martins, W.C.; Reginato, C.; Parada, E.; Egea, J.; López, M.G.; Tasca, C.I. Guanosine controls inflammatory pathways to afford neuroprotection of hippocampal slices under oxygen and glucose deprivation conditions. *J. Neurochem.* **2013**, *126*, 437–450. [CrossRef] [PubMed]

12.   Traversa, U.; Bombi, G.; Di Iorio, P.; Ciccarelli, R.; Werstiuk, E.S.; Rathbone, M.P. Specific [(3)H]-guanosine binding sites in rat brain membranes. *Br. J. Pharmacol.* **2002**, *135*, 969–976. [CrossRef] [PubMed]

13.   Traversa, U.; Bombi, G.; Camaioni, E.; Macchiarulo, A.; Costantino, G.; Palmieri, C.; Caciagli, F.; Pellicciari, R. Rat brain guanosine binding site. Biological studies and pseudo-receptor construction. *Bioorganic Med. Chem.* **2003**, *11*, 5417–5425. [CrossRef] [PubMed]

14.   Volpini, R.; Marucci, G.; Buccioni, M.; Dal Ben, D.; Lambertucci, C.; Lammi, C.; Mishra, R.C.; Thomas, A.; Cristalli, G. Evidence for the existence of a specific g protein-coupled receptor activated by guanosine. *ChemMedChem* **2011**, *6*, 1074–1080. [CrossRef] [PubMed]

15.   Dal-Cim, T.; Poluceno, G.G.; Lanznaster, D.; de Oliveira, K.A.; Nedel, C.B.; Tasca, C.I. Guanosine prevents oxidative damage and glutamate uptake impairment induced by oxygen/glucose deprivation in cortical astrocyte cultures: Involvement of A1 and A2A adenosine receptors and PI3K, MEK, and PKC pathways. *Purinergic Signal.* **2019**, in press. [CrossRef]

16.   Ciruela, F. Guanosine behind the scene. *J. Neurochem.* **2013**, *126*, 425–427. [CrossRef]

17.   Ciruela, F.; Casadó, V.; Rodrigues, R.J.; Luján, R.; Burgueño, J.; Canals, M.; Borycz, J.; Rebola, N.; Goldberg, S.R.; Mallol, J.; et al. Presynaptic control of striatal glutamatergic neurotransmission by adenosine A1-A2Areceptor heteromers. *J. Neurosci.* **2006**, *26*, 2080–2087. [CrossRef]

18.   Ciruela, F.; Ferre, S.; Casado, V.; Cortes, A.; Cunha, R.A.; Lluis, C.; Franco, R. Heterodimeric adenosine receptors: A device to regulate neurotransmitter release. *Cell. Mol. Life Sci.* **2006**, *63*, 2427–2431. [CrossRef]

19.   Duroux, R.; Ciancetta, A.; Mannes, P.; Yu, J.; Boyapati, S.; Gizewski, E.; Yous, S.; Ciruela, F.; Auchampach, J.A.; Gao, Z.-G.; et al. Bitopic fluorescent antagonists of the A2A adenosine receptor based on pyrazolo[4,3-: E] [1,2,4]triazolo[1,5- c] pyrimidin-5-amine functionalized congeners. *MedChemComm* **2017**, *8*, 1659–1667. [CrossRef]

20.   Ledent, C.; Vaugeois, J.M.; Schiffmann, S.N.; Pedrazzini, T.; El Yacoubi, M.; Vanderhaeghen, J.J.; Costentin, J.; Heath, J.K.; Vassart, G.; Parmentier, M. Aggressiveness, hypoalgesia and high blood pressure in mice lacking the adenosine A2a receptor. *Nature* **1997**, *388*, 674–678. [CrossRef]

21.   Clark, J.D.; Gebhart, G.F.; Gonder, J.C.; Keeling, M.E.; Kohn, D.F. Special report: The 1996 guide for the care and use of laboratory animals. *Ilar J. /Natl. Res. Counc. Inst. Lab. Anim. Resour.* **1997**, *38*, 41–48. [CrossRef] [PubMed]

22.   Liu, Y.; Peterson, D.A.; Kimura, H.; Schubert, D. Mechanism of cellular 3-(4,5-dimethylthiazol-2-yl)-2,5-diphenyltetrazolium bromide (MTT) reduction. *J. Neurochem.* **1997**, *69*, 581–593. [CrossRef] [PubMed]

23. Ferreira, A.G.K.; da Cunha, A.A.; Machado, F.R.; Pederzolli, C.D.; Dalazen, G.R.; de Assis, A.M.; Lamers, M.L.; dos Santos, M.F.; Dutra-Filho, C.S.; Wyse, A.T.S. Experimental hyperprolinemia induces mild oxidative stress, metabolic changes, and tissue adaptation in rat liver. *J. Cell. Biochem.* **2012**, *113*, 174–183. [CrossRef] [PubMed]

24. Fernandez-Duenas, V.; Gomez-Soler, M.; Jacobson, K.A.; Kumar, S.T.; Fuxe, K.; Borroto-Escuela, D.O.; Ciruela, F. Molecular determinants of A(2A) R-D(2) R allosterism: Role of the intracellular loop 3 of the D(2) R. *J. Neurochem.* **2012**, *123*, 373–384. [CrossRef]

25. Stoddart, L.A.; Johnstone, E.K.M.; Wheal, A.J.; Goulding, J.; Robers, M.B.; Machleidt, T.; Wood, K.V.; Hill, S.J.; Pfleger, K.D.G. Application of BRET to monitor ligand binding to GPCRs. *Nat. Methods* **2015**, *12*, 661–663. [CrossRef]

26. Taura, J.; Fernández-Dueñas, V.; Ciruela, F. Determination of GPCR-mediated cAMP accumulation in rat striatal synaptosomes. *Neuromethods* **2016**, *110*, 455–464.

27. Borroto-Escuela, D.O.; Romero-Fernandez, W.; Tarakanov, A.O.; Ciruela, F.; Agnati, L.F.; Fuxe, K. On the existence of a possible A2A-D2-beta-Arrestin2 complex: A2A agonist modulation of D2 agonist-induced beta-arrestin2 recruitment. *J. Mol. Biol.* **2011**, *406*, 687–699. [CrossRef]

28. Xu, Y.; Xie, X.; Duan, Y.; Wang, L.; Cheng, Z.; Cheng, J. A review of impedance measurements of whole cells. *Biosens. Bioelectron.* **2016**, *77*, 824–836. [CrossRef]

29. Hillger, J.M.; Schoop, J.; Boomsma, D.I.; Slagboom, P.E.; IJzerman, A.P.; Heitman, L.H. Whole-cell biosensor for label-free detection of GPCR-mediated drug responses in personal cell lines. *Biosens. Bioelectron.* **2015**, *74*, 233–242. [CrossRef]

30. Stallaert, W.; Dorn, J.F.; van der Westhuizen, E.; Audet, M.; Bouvier, M. Impedance responses reveal β_2-adrenergic receptor signaling pluridimensionality and allow classification of ligands with distinct signaling profiles. *PLoS ONE* **2012**, *7*, e29420. [CrossRef]

31. Fernández-Dueñas, V.; Taura, J.J.; Cottet, M.; Gómez-Soler, M.; López-Cano, M.; Ledent, C.; Watanabe, M.; Trinquet, E.; Pin, J.-P.; Luján, R.; et al. Untangling dopamine-adenosine receptor-receptor assembly in experimental parkinsonism in rats. *Dis. Models Mech.* **2015**, *8*, 57–63. [CrossRef] [PubMed]

32. Thomaz, D.T.; Dal-Cim, T.A.; Martins, W.C.; Cunha, M.P.; Lanznaster, D.; de Bem, A.F.; Tasca, C.I. Guanosine prevents nitroxidative stress and recovers mitochondrial membrane potential disruption in hippocampal slices subjected to oxygen/glucose deprivation. *Purinergic Signal.* **2016**, *12*, 707–718. [CrossRef] [PubMed]

33. Tasca, C.I.; Lanznaster, D.; Oliveira, K.A.; Fernández-Dueñas, V.; Ciruela, F. Neuromodulatory effects of guanine-based purines in health and disease. *Front. Cell. Neurosci.* **2018**, *12*, 376. [CrossRef] [PubMed]

34. Núñez, F.; Taura, J.; Camacho, J.; López-Cano, M.; Fernández-Dueñas, V.; Castro, N.; Castro, J.; Ciruela, F. PBF509, an Adenosine A2A Receptor Antagonist with Efficacy in Rodent Models of Movement Disorders. *Front. Pharmacol.* **2018**, *9*, 1200. [CrossRef]

35. Almeida, R.F.; Comasseto, D.D.; Ramos, D.B.; Hansel, G.; Zimmer, E.R.; Loureiro, S.O.; Ganzella, M.; Souza, D.O. Guanosine Anxiolytic-Like Effect Involves Adenosinergic and Glutamatergic Neurotransmitter Systems. *Mol. Neurobiol.* **2017**, *54*, 423–436. [CrossRef]

36. Dobrachinski, F.; Gerbatin, R.R.; Sartori, G.; Golombieski, R.M.; Antoniazzi, A.; Nogueira, C.W.; Royes, L.F.; Fighera, M.R.; Porciúncula, L.O.; Cunha, R.A.; et al. Guanosine Attenuates Behavioral Deficits After Traumatic Brain Injury by Modulation of Adenosinergic Receptors. *Mol. Neurobiol.* **2019**, *56*, 3145–3158. [CrossRef]

37. Ciruela, F.; Gómez-Soler, M.; Guidolin, D.; Borroto-Escuela, D.O.; Agnati, L.F.; Fuxe, K.; Fernández-Dueñas, V. Adenosine receptor containing oligomers: Their role in the control of dopamine and glutamate neurotransmission in the brain. *Biochim. Biophys. Acta Biomembr.* **2011**, *1808*, 1245–1255. [CrossRef]

38. Ferré, S.; Casadó, V.; Devi, L.A.; Filizola, M.; Jockers, R.; Lohse, M.J.; Milligan, G.; Pin, J.-P.; Guitart, X. G Protein–Coupled Receptor Oligomerization Revisited: Functional and Pharmacological Perspectives. *Pharmacol. Rev.* **2014**, *66*, 413–434. [CrossRef]

39. Orru, M.; Bakešová, J.; Brugarolas, M.; Quiroz, C.; Beaumont, V.; Goldberg, S.R.; Lluís, C.; Cortés, A.; Franco, R.; Casadó, V.; et al. Striatal pre- and postsynaptic profile of adenosine A2A receptor antagonists. *PLoS ONE* **2011**, *6*, e16088. [CrossRef]

40. Navarro, G.; Cordomí, A.; Brugarolas, M.; Moreno, E.; Aguinaga, D.; Pérez-Benito, L.; Ferre, S.; Cortés, A.; Casadó, V.; Mallol, J.; et al. Cross-communication between G i and G s in a G-protein-coupled receptor heterotetramer guided by a receptor C-terminal domain. *BMC Biol.* **2018**, *16*, 24. [CrossRef]

41. Ciruela, F.; Fernández-Dueñas, V. GPCR oligomerization analysis by means of BRET and dFRAP. In *G Protein-Coupled Receptor Screening Assays*; Humana Press: New York, NY, USA, 2015.